Journal Name

Dynamic Article Links ►

SAND2012-9333J

Cite this: DOI: 10.1039/c0xx00000x

www.rsc.org/xxxxxx

ARTICLE TYPE

Microfluidic platforms for RNA interference screening of virus-host interactions

Benjamin R. Schudel, Brooke Harmon, Vinay V. Abhyankar, Benjamin W. Pruitt, Oscar A. Negrete*, and Anup K. Singh*

Received (in XXX, XXX) Xth XXXXXXXXX 20XX, Accepted Xth XXXXXXXXX 20XX
DOI: 10.1039/b000000x

RNA interference (RNAi) is a powerful tool for functional genomics with the capacity to comprehensively analyze host-pathogen interactions. High-throughput RNAi screening is used to systematically perturb cellular pathways and discover therapeutic targets, but the method can be tedious and requires extensive capital equipment and expensive reagents. To aid in the development of an inexpensive miniaturized RNAi screening platform, we have developed a two part microfluidic system for patterning and screening gene targets on-chip to examine cellular pathways involved in virus entry and infection. First, a multilayer polydimethylsiloxane (PDMS)-based spotting device was used to array siRNA molecules into 96 microwells targeting markers of endocytosis, along with siRNA controls. By using a PDMS-based spotting device, we remove the need for a microarray printer necessary to perform previously described small scale (e.g. cellular microarrays) and microchip-based RNAi screening, while still minimizing reagent usage tenfold compared to conventional screening. Second, the siRNA spotted array was transferred to a reversibly sealed PDMS-based screening platform containing microchannels designed to enable efficient cell loading and transfection of mammalian cells while preventing cross-contamination between experimental conditions. Validation of the screening platform was examined using Vesicular stomatitis virus and emerging pathogen Rift Valley fever virus, which demonstrated virus entry pathways of clathrin-mediated endocytosis and caveolae-mediated endocytosis, respectively. The techniques here are adaptable to other well-characterized infection pathways with a potential for large scale screening in high containment biosafety laboratories.

Introduction

Emerging pathogens such as Rift Valley fever virus (RVFV) which causes hemorrhagic fever, pose a serious public health threat due to the lack of treatments or vaccines for these diseases.[1, 2] RNA interference (RNAi) is a powerful functional genetic approach used to elucidate cellular factors involved in host-pathogen interactions and to provide potential targets for therapeutic intervention.[3, 4] RNAi is typically achieved using chemically synthesized small interfering RNAs (siRNAs) which are double-stranded RNAs targeted to a specific gene. Introduced by transfection into a cell, siRNAs induce gene silencing thereby reducing or eliminating protein expression. As viruses exploit cellular proteins to initiate infection and complete their life cycle, genome-wide libraries of siRNAs can be used to determine, in principle, all genes in a given host cell that either promote or inhibit infection.[5] Although genome-wide RNAi represents a robust systems biology approach to comprehensive host-pathogen analysis and therapeutic target discovery, its use in studying emerging viruses that require high-level biocontainment facilities is limited. To date, no genome-wide RNAi studies involving BSL-4 pathogens have been published and only one study using West Nile virus (a BSL-3 agent) has been reported.[6] RNAi libraries and reagents are expensive, and a burdensome coordination exists between high-throughput screening (HTS) equipment with virus and high-level biocontainment (e.g. BSL-3 or BSL-4). This prevents widespread use of RNAi screening against highly pathogenic viruses. To take full advantage of RNAi screening for agents such as RVFV, alternative platforms amenable to the study of virus-host interactions in high biocontainment facilities need development.

RNAi screening on microscale platforms offer significant advantages over traditional microtiter plate assays used in HTS, and includes a portability feature that would facilitate screening in high-containment laboratories. One of the first small scale RNAi screening platforms described was transfection cellular microarrays. These RNAi cellular microarrays contain spots of siRNA reagents printed on glass slides where cells grown directly over these spots are transfected.[7, 8] Although cellular microarrays minimize reagent consumption and limit the need of robotic HTS equipment, uncontrolled cell seeding results in wide cell number variability per spot and the lack of defined borders between cells can cause cross-contamination between spots, thus complicating data analysis and deterring widespread use of this platform. More recently, efforts to improve miniaturized RNAi screening using microfluidic lab-on-a-chip technology have been described.[9-11]

Applications of microfluidic chip architecture to cell culture studies have led to a host of new cellular studies that exploit the physics of the microscale.[12-14] Microfluidic-based mammalian cell culture assays include studies on adherent cell manipulation,[15] 3D microenvironments,[16] gene expression,[17] and controlled infection.[18] With respect to on-chip transfection capabilities, previous studies have looked at oligonucleotide delivery,[19] utilization of microdroplets,[20] and electroporation.[21] One promising lab-on-a-chip platform utilizes a microwell array on an electroporation-ready transparent substrate, thereby circumventing previous issues regarding spot cross-contamination, while also being applicable to primary cells notoriously known for their transfection difficulty.[11] However, all previously described cellular microarray and microchip-based methods use an open cell culture, where cell media and secreted cellular factors are shared between different experimental conditions. For miniaturized RNAi platforms involving virus infection, internal design features are necessary to prevent cross-contamination of secreted soluble factors from infected cells.

To advance the current state of self-contained portable bioscreening platforms for virus-host interaction studies, we have developed an integrated RNAi screening platform benefiting from low reagent volumes, simple fabrication, and rapid scale up. Our platform was specifically designed to screen for viral endocytosis pathways as a proof-of-principle demonstration for general infection pathway characterization that sets the stage for future genome-wide RNAi screening studies. Our PDMS based microfluidic RNAi screening method is comprised of a two-part system for (i) patterning siRNA molecules and (ii) screening gene targets on-chip. With this platform, we confirm RVFV entry is mediated through caveolae-mediated endocytosis while Vesicular stomatitis virus (VSV) enters cells through clathrin-mediated endocytosis.

Experimental

Microfabrication and design

Glass slides [75mm x 25mm] were etched to create 96 microwells 50 μm deep and 500 μm wide, with intrawell spacing of 800 μm in the x-direction and 1.125 mm in the y-direction [Caliper] [Figure 1]. These etched microwells were then aligned to PDMS-based devices containing microchannels that were cast using standard soft lithography techniques [mask design available in Supplementary Figure 1].[22] The etched glass slides and PDMS devices were sterilized in an autoclave at 120°C for 30 minutes prior to assembly in a biosafety cabinet.

siRNA spotting

After alignment to microwells, PDMS-based devices were placed in a desiccation unit under vacuum for 1 hr to evacuate the PDMS bulk and prevent bubble formation within the microchannels.[23] 1 uL of the transfection mix for RNAi screening, as prepared in previous cellular microarray protocols [2 μL Lipofectamine 2000, 3 μL 0.4 M sucrose in Opti-MEM, 5 μL 20 μM pooled siRNA, 7 μL 0.2% w/v gelatin, 0.01% v/v fibronectin],[8] was pipetted onto the individual channel input ports and pulled into the channels via vacuum actuation of the evacuation lines [Supplementary movie 1]. These small evacuation lines were designed similarly to valves in multilayer soft lithography.[24] However, these lines were small enough to not act as valves, so that when actuated under negative pressure the transfection mix would be loaded into the microchannels and fill the geometries of the microwells with minimal dead volume. The lanes were then dried within the device for 24-72 hr in a closed desiccation chamber at atmospheric pressure with aluminosilicate drying pearls [Sigma]. The siRNAs used for the experiment include AllStars Neg-22 (scrambled), GFP-22, AlexaFluor548 (red-labeled scrambled, for demonstration of transfection); and single siRNAs selected from pools including: CAV1_7, DMN2_12, CLTC_13, PAK1_8, PI3K_10, and EPS15_1 [Qiagen]. We previously demonstrated that this particular set of siRNAs was capable of dissecting viral endocytosis entry pathways.[25] The device was then removed from the desiccation unit and peeled back from the glass surface under sterile conditions, leaving behind the patterned gelatin-stabilized transfection mix in the microwells in orderly rows on the microscope slide.

Screening assembly and transfection

The patterned siRNA slide was aligned to a PDMS-based screening platform designed to accommodate cell loading, transfection and virus loading. The assembled platform was placed within a vacuum desiccator for 1 hr in order to degas the PDMS bulk and prevent bubble formation upon introduction of cell solution. HeLa cells were incubated in cell culture dishes until 90% confluency, then trypsinized and centrifuged at 2400 RPM for 5 minutes. Excess media was removed from the final pellet, which was resuspended in Dulbecco's Modified Eagle Medium (DMEM) containing 15% v/v fetal bovine serum (FBS) and 1% v/v penicillin/streptomycin (P/S). The cell suspension (40 cells nL^{-1}) was introduced via pipette in 5 μL increments into ports of the microfluidic screening platform. HeLa cells settled into the microwells when media flow was stopped and entrance and exit droplets were merged under a liquid media cap.[26]

Four hours after cell seeding, fresh media was introduced via pipette, taking care to ensure the inlets and outlets remained wet at all times to prevent the introduction of bubbles into the platform. After visual inspection of the platform, the setup was then placed in the incubator for an additional 20-68 hrs. For optimization experiments utilizing only GFP-22 and scrambled siRNA, cells were infected 24 hr post-transfection. For experiments knocking down expression of genes involved in endocytosis, cells were infected 72 hr post-transfection. This increase in transfection time allowed for downregulation of endocytosis markers at the protein level.[25] For the duration of the 4-day experiment (72 hr transfection, 24 hr infection), fresh media was injected by pipette into the chambers once per 24 hours. Finally, 1 mL of media was added to the surface of the microfluidic platform after each injection onto the platform. This media cap was utilized between media refreshment to ensure the platform did not dry out.

Virus entry

The reporter viruses used in this assay were RVFV strain MP12 and VSV, which were specifically engineered to express GFP only upon infection.[27, 28] RVFV is a NIH category A priority pathogen because of its potential use as a biological weapon, and experiments using pathogenic strains of RVFV have to be performed in high-level biosafety containment labs, whereas RVFV MP12 can be handled at BSL-2 biocontainment. RVFV strain MP12 was derived from the Egyptian strain ZH548 by

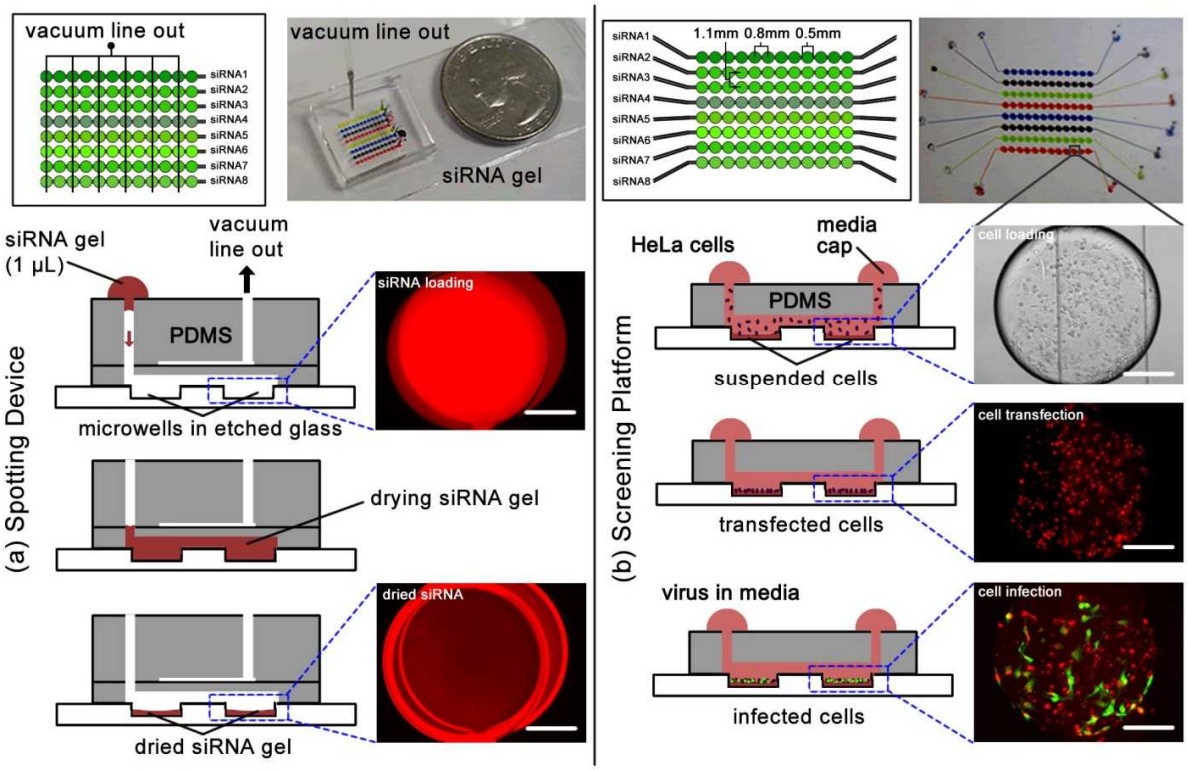

Figure 1. Schematic for microfluidic spotting devices and genetic screening platform with microwell images. (a) The sterilized microfluidic spotting device is aligned to a glass microscope slide with 96 etched wells. Alexa 538 conjugated control siRNA is loaded into the wells via vacuum actuation. The device is dried in a desiccation chamber for 1-2 days, leaving behind gelatin-stabilized transfection reagent and siRNA. (b) The spotting device is removed and the slide is aligned to a microfluidic screening platform. The platform is then loaded with HeLa cells [40 nL^{-1}]. After 1-3 days of transfection, the cells uptake the siRNA. GFP expressing virus upon infection is injected through the media lines for infection. The microwells of the platform are imaged at right, corresponding to each step in the screen. Scale bars are 100 µm.

propagation for 12 serial tissue culture passages in the presence of the mutagenic agent 5-fluorouracil creating an attenuated virus used as a vaccine.[29] When loading cells at a concentration of 40 cells nL^{-1}, approximately ~300 cells/well (324 ± 21, n=100 wells) settled into each well and were reverse transfected with siRNA. Infection with RVFV or VSV was performed at a virus concentration of 10^6 infectious units/mL and equal to a multiplicity of infection (MOI) of approximately ~0.2. The virus containing media solution was introduced to the cells using the same method as the media replenishment. Devices were then placed into an incubator at 37°C, 5% CO2. The platform was imaged for GFP at 14 hr and 24 hr for VSV and RVFV, respectively.

Image collection and analysis

The screening platform was placed onto an Olympus IX70 inverted microscope. Fluorescent and brightfield images were collected for each microwell using a GFP filter cube and 10X objective. The images were collected using a Hamamatsu C10600-10B (ORCA-R2) digital camera. Each of these pictures was analysed using ImageJ, with an in-house modified cell counting module (plugin application available upon request). For each experiment, a threshold value above background was chosen. All images have this background applied, and pixels are binned above threshold. Each set of pixels is marked and grouped according to suggested cell size, and cells are counted for final analysis. Relative infection was determined by dividing the number infected cells (GFP expressing cells) by the number of infected cells in wells containing scrambled siRNA (negative control). Statistical significance is also calculated against the negative control condition for each set of experiments.

Results and discussion

With the goal of creating an inexpensive, portable and miniaturized RNAi screening platform for studying virus-host interactions, we set out to integrate microfluidic devices within an existing cellular microarray format. Published protocols have outlined techniques to create siRNA transfection arrays on glass slides using a microarray printer for reagent patterning.[8] However, since cell microarrays lack physical barriers to confine cell location, inter-spot migration of transfection cells leads to cross-contamination and confounds phenotypic analysis. Moreover, without these physical barriers, it is difficult to identify with absolute accuracy the individual spot location during image analysis. To improve on these cellular microarray techniques, glass slides were first etched with 500µM diameter microwells in a 96 well format with a density of 120 microwells/cm^2 [Figure 1]. Microwells offer advantages of not only spatially confining cell cultures preventing cross contamination between transfected cells, but they provide a physical marker used for end-point analysis through imaging. Additionally, to remove the capital expense of a microarray printer while still using low reagent volumes, a microfluidic spotting device was developed using PDMS-based soft lithography techniques [Figure 1a].

The microfluidic spotting device was designed as a two-layer device, to aliquot small samples of viscous transfection mix across microwells in a controlled fashion. The bottom layer contained eight individually addressable, 40 µm wide microfluidic channels running in parallel that were each aligned over a row of 12 microwells. A second PDMS layer contained small evacuation lines running perpendicular to the microfluidic channels. When the lines were actuated under negative pressure (~250 mTorr) the air within the lower channels was evacuated and the reagents were loaded into the channel [suppl. movie 1]. This important design feature minimized reagent dead volumes and therefore reduced waste of expensive transfection reagents and siRNA libraries. Consumption of the siRNAs in our technique is over 10-fold less than with traditional HTS in 384-well plates (1 ng siRNA/microwell vs. 10 ng/ well). After the slide was spotted and siRNAs were dried, the reversibly sealed microfluidic spotting device was removed and a microfluidic screening platform containing a new set of microfluidic channels was aligned over the microwells. siRNAs dried onto a glass surface using gelatin-stabilized spots have been demonstrated to be stable for up to 15 months.[8] Therefore, once the second device is aligned and reversibly sealed, the microfluidic RNAi screening platform with dried siRNA becomes a stable transfection-ready platform.

The microfluidic screening platform was designed as a single layer device with eight individually addressable, 300 µm wide microfluidic channels running in parallel along rows of 12 microwells containing dried siRNA regents [Figure 1b]. This network of microfluidic channels guides fluid flow for simplified cell and virus loading that can be pumped using pipettes without producing shear stress strong enough to destroy cells within the microwells. Previous cellular microarray designs use an open cell seeding technique that does not control cell seeding per spot, but instead relies on the growth of a layer of confluent cells leaving a majority of the cells untransfected. This open seeding method creates variability in cells per spot and the large number of untransfected cells creates a large waste of cells and could be cost prohibitive when using primary cells. Also, our microfluidic design simplifies cell seeding as compared to other methods that require individually seeding of microwell spots up to ~10000 per plate.[30] Lastly, the microfluidic screening device adds a novel feature in microscale RNAi technology since it is the first, to our knowledge, designed to prevent cross contamination of experimental media conditions and soluble factors, important for regulating infectious dose or for isolation of negative (no virus) controls.

As proof-of-principle, experiments with validated siRNA controls were performed. Using the siRNA reverse transfection formulation previously described for cellular microarrays,[8] a positive control of siRNA targeting GFP and a scrambled siRNA negative control were each spotted into two lanes with 12 microwells per lane in the microfluidic platform. HeLa cells were then seeded and subsequently reverse transfected for 24 hr. A schematic of the siRNA control experiments is shown Figure 2a. The HeLa cells were then infected with recombinant RVFV MP-12 that expresses the reporter GFP upon infection and replication. Fluorescence images of GFP expression were then taken and analysed by image processing [Figure 2a]. The scrambled siRNA

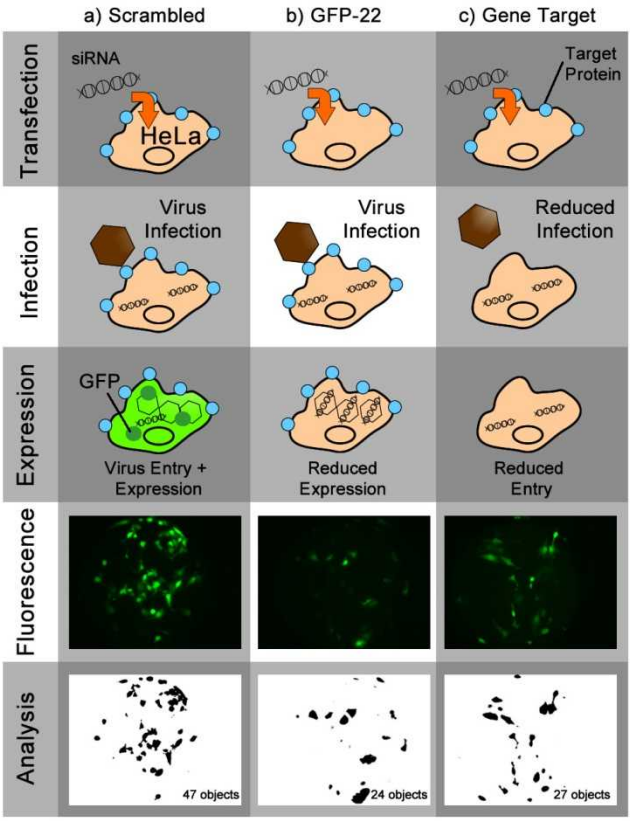

Figure 2. Schematic of on-chip RNAi methodology for virus screening using siRNA controls and specific gene targets. The assay utilizes GFP-producing virus, which expresses GFP upon infection in cells. (a) As a negative control, scrambled (non-specific) siRNA is transfected into HeLa cells and upon infection, GFP expression is *not* blocked. (b) As a positive control, HeLa cells are transfected with siRNA targeted against the GFP gene, which reduced GFP expression. (c) Lastly, targeting a host gene necessary for virus entry or replication will reduce the number of cells infected and limit GFP expression as compared to the negative control. Representative microwells fluorescence images are shown for each siRNA condition. Green cells are counted in individual microwells by threshold image analysis to quantify the amount of cells infected in a given condition and normalized to the amount of cells infected in the scrambled control. Scale bars are 100 µm.

in the negative control experiment does not target a viral or human cell gene, therefore RVFV infection and GFP expression are unaffected. In contrast, siRNAs that target the GFP gene expressed by the virus after entry and replication limit the number of GFP expressing cells as compared to the negative control [Figure 2b]. Relative infection was determined by dividing the number infected cells (GFP expressing cells) in wells containing GFP-22 siRNA (positive control) by the number of infected cells in wells containing scrambled siRNA (negative control).

To test the microfluidic screening platform targeting cellular host proteins [Figure 2c], siRNAs that inhibit virus entry pathways were used. Viruses that enter cells through pH-dependent means typically utilize one of the major endocytic cellular pathways that include clathrin-mediated endocytosis (CME), caveolae-mediated endocytosis (CavME), and macropinocytosis.[31] Each of these endocytic pathways can be knocked out by silencing gene expression of regulators involved either in the structural assembly of the endocytic vesicles or in signaling events required for endocytosis activation. As we have previously demonstrated, CavME was inhibited by RNAi

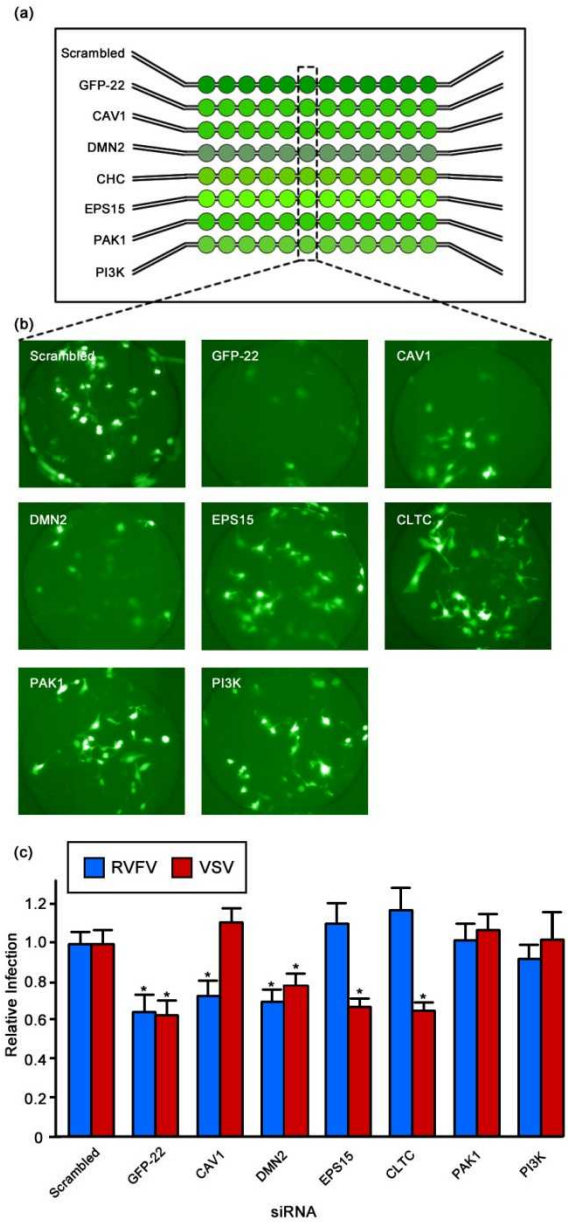

Figure 3. Virus entry pathway analysis via microfluidic RNAi screening. (a) A schematic of siRNA patterning within 96-microwell screening platform targeting genes involved in endocytosis pathways is shown. siRNAs targeting CavME are caveolin-1 (CAV1) and dynamin II (DMN2), those that target CME are against DMN2, epidermal growth factor receptor pathway substrate 15 (EPS15) and clathrin heavy chain (CLTC), while those that target macropinocytosis are against p21 activated kinase 1 (PAK1) and phosphoinositide-3-kinase (PI3K). siRNAs targeting GFP (GFP-22) and scramble negative control is included. Each gene-target is replicated twelve times within the device. (b) Representative fluorescent images of HeLa cells transfected with the siRNAs on chip and subsequently infected with RVFV-GFP. (c) Average relative infection of siRNA transfected HeLa cells with RVFV and VSV compared to scrambled siRNA control (± standard deviation) is shown. *Statistically significant from scrambled control ($p<0.05$).

targeting structural components of caveolae including caveolin-1 (CAV1) and dynamin II (DMN2), CME was inhibited through clathrin heavy chain (CLTC), epidermal growth factor receptor pathway substrate 15 (EPS15) and DMN2 gene silencing, while macropinocytosis was blocked by inhibition of signaling events by kinases p21 activated kinase (PAK1) and phosphoinositide-3-kinase (PI3K).[25] These targets were considered ideal for a virus entry validation of the screen, with both VSV and RVFV selected to demonstrate two of the three types of viral infection [Figure 3].

Using the microfluidic spotting device, siRNAs targeting CAV1, DMN2, EPS15, CLTC, PAK1 and PI3K were spotted into the microwells with one target per lane. Additionally, siRNAs targeting GFP expression (GFP-22) (positive control) and a scrambled negative control (Scrambled) were filled into the remaining two lanes of a single device [Figure 3a]. HeLa cells were reverse transfected for 72 hr to allow for maximum silencing at the protein level, then infected with either RVFV or VSV and subsequently imaged under optimized parameters as described in Experimental [Figure 3b]. RVFV infection was inhibited by siRNAs targeting CAV-1 and DMN2, as well as by the positive control of siRNA to GFP (GFP-22). In contrast, the level of RVFV infection (GFP expression) did not vary between the negative control siRNA and EPS15, CLTC, PAK1, or PI3K. These trends were consistent across the microwells in a lane and reproducible between chip experiments, with an average inhibition of infection of 26.9% ±7.6 by CAV1 siRNA and 29.9% ± 5.7 by DMN2 siRNA relative to the negative control [Figure 3c, blue bars]. VSV infection was significantly inhibited by siRNA targeting DMN2, EPS15 and CLTC, but not CAV1, PAK1 or PI3K [Figure 3c, red bars].

This microfluidic screening method was able to attain these results using very low reagent volumes, as well as being self-contained in a highly portable device suitable for use in high containment labs. Without the use of external robotics, the entire screening method can be contained in a biosafety cabinet, while still attaining accuracy through repetition all on-chip. This microfluidic method also has the capability of scaling up to larger devices, which could be utilized for genome-wide screening.

Conclusions

We have demonstrated a microfluidic method for RNAi screening of virus-host interactions. The microfluidic design has several advantages as compared to conventional HTS screening in microplate format and has enhancements to previously described cellular microarray technologies, such as portability and low reagent usage. The microfluidic platform provides a method for production of transfection cell arrays with sample densities allowing screening of 120 spots/cm^2 or up to 2250 per glass slide. Consumption of the siRNAs in our technique is over 10-fold less than with traditional HTS in 384-well plates (1 ng siRNA/microwell vs. 10 ng/well). However, the PDMS spotting device removes the need for a microarrayer necessary to print RNAi spots for cellular microarray technologies. Also, as compared to most of the cell microarray methods, where a lawn of cells is laid across the whole array,[8, 32, 33] our microfluidic platform provides a simplified method for achieving a patterned array layout, where cells are efficiently used and not wasted. This feature is important when considering screening with limited populations (e.g. primary cells). Also, the microwell configuration facilitates the quality control and image analysis as cells in different experimental conditions are physically separated creating an end-point analysis through imaging without possibility for sample mixing between microchannel positions.

Since in this method cells are seeded in a controlled manner through microchannels, well-to-well variability inherent in classical HTS systems is reduced in the microfluidic screening device, potentially increasing the accuracy of RNAi screens.

RVFV and VSV were utilized here to demonstrate the use of microfluidic platforms for systematic RNAi screening. Here, we verify that RVFV enters through CavME by inhibiting infection with siRNAs targeting CAV1 and DMN2 on the RNAi virus entry microfluidic platform. Similarly, we show that VSV, a virus that undergoes CME dependent entry, had a reduction in infection when the genes associated with CME were knocked down (EPS15, DMN2 and CLTC) in the microfluidic device. These results were specific as RVFV was not inhibited by knockdown of regulators specific for CME or macropinocytosis and VSV was not inhibited by regulators specific for CavME (CAV1) or macropinocytosis (PAK1 and PI3K). Our results show that the present RNAi platform provides a rapid, simplified and standalone method for virus entry pathways analysis, thereby providing valuable insight into host-pathogen interactions and potential therapeutic targets. Future studies will enable these microscale devices to enter high-containment laboratories to validate these entry results with highly pathogenic viral strains.

Acknowledgements

Sandia National Laboratories is a multi-program laboratory managed and operated by Sandia Corporation, a wholly owned subsidiary of Lockheed Martin Corporation, for the U.S. Department of Energy's National Nuclear Security Administration under contract DE-AC04-94AL85000. This work was supported by a Laboratory Directed Research and Development grant given to O.A.N. at Sandia National Laboratories.

The authors would like to acknowledge Tetsuro Ikegami at the University of Texas Medical Branch for the RVFV MP12 GFP strain.

Notes and references

Sandia National Laboratories, Department of Biotechnology and Bioengineering, P.O. Box 969, Livermore, CA 94551. E-mail: onegret@sandia.gov or aksingh@sandia.gov

† Electronic Supplementary Information (ESI) available: [details of any supplementary information available should be included here]. See DOI: 10.1039/b000000x/

1. K. E. Jones, N. G. Patel, M. A. Levy, A. Storeygard, D. Balk, J. L. Gittleman and P. Daszak, *Nature*, 2008, **451**, 990-993.
2. S. C. Weaver and W. K. Reisen, *Antiviral research*, 2010, **85**, 328-345.
3. A. L. Brass, D. M. Dykxhoorn, Y. Benita, N. Yan, A. Engelman, R. J. Xavier, J. Lieberman and S. J. Elledge, *Science*, 2008, **319**, 921-926.
4. R. Konig, S. Stertz, Y. Zhou, A. Inoue, H. H. Hoffmann, S. Bhattacharyya, J. G. Alamares, D. M. Tscherne, M. B. Ortigoza, Y. Liang, Q. Gao, S. E. Andrews, S. Bandyopadhyay, P. De Jesus, B. P. Tu, L. Pache, C. Shih, A. Orth, G. Bonamy, L. Miraglia, T. Ideker, A. Garcia-Sastre, J. A. Young, P. Palese, M. L. Shaw and S. K. Chanda, *Nature*, 2010, **463**, 813-817.
5. S. Cherry, *Current opinion in microbiology*, 2009, **12**, 446-452.
6. M. N. Krishnan, A. Ng, B. Sukumaran, F. D. Gilfoy, P. D. Uchil, H. Sultana, A. L. Brass, R. Adametz, M. Tsui, F. Qian, R. R. Montgomery, S. Lev, P. W. Mason, R. A. Koski, S. J. Elledge, R. J. Xavier, H. Agaisse and E. Fikrig, *Nature*, 2008, **455**, 242-245.
7. D. B. Wheeler, A. E. Carpenter and D. M. Sabatini, *Nat Genet Suppl*, 2005, **37**, S25-30.
8. H. Erfle, B. Neumann, U. Liebel, P. Rogers, M. Held, T. Walter, J. Ellenberg and R. Pepperkok, *Nature protocols*, 2007, **2**, 392-399.
9. T. Jain, R. McBride, S. Head and E. Saez, *Lab Chip*, 2009, **9**, 3557-3566.
10. H. Huang, Z. Wei, Y. Huang, D. Zhao, L. Zheng, T. Cai, M. Wu, W. Wang, X. Ding, Z. Zhou, Q. Du, Z. Li and Z. Liang, *Lab Chip*, 2011, **11**, 163-172.
11. T. Jain, A. Papas, A. Jadhav, R. McBride and E. Saez, *Lab on a Chip*, 2012, **12**.
12. E. W. Young and D. J. Beebe, *Chemical Society reviews*, 2010, **39**, 1036-1048.
13. K. R. King, S. Wang, D. Irimia, A. Jayaraman, M. Toner and M. L. Yarmush, *Lab Chip*, 2007, **7**, 77-85.
14. T. M. Squires and S. R. Quake, *Reviews of Modern Physics*, 2005, **77**, 977-1026.
15. V. Starkuviene and R. Pepperkok, *British journal of pharmacology*, 2007, **152**, 62-71.
16. J. Lii, W.-J. Hsu, H. Parsa, A. Das, R. Rouse and S. K. Sia, *Analytical chemistry*, 2008, **80**, 3640-3647.
17. N. M. Toriello, E. S. Douglas, N. Thaitrong, S. C. Hsiao, M. B. Francis, C. R. Bertozzi and R. A. Mathies, *Proceedings of the National Academy of Sciences of the United States of America*, 2008, **105**, 20173-20178.
18. G. M. Walker, M. S. Ozers and D. J. Beebe, *Sensors and Actuators B: Chemical*, 2003, **98**, 347-355.
19. B. Yu, J. Zhu, W. Xue, Y. Wu, X. Huang, L. J. Lee and R. J. Lee, *Anticancer Research*, 2011, **31**, 771-776.
20. H. Hufnagel, A. Huebner, C. Gulch, K. Guse, C. Abell and F. Hollfelder, *Lab on a Chip*, 2009, **9**, 1576-1582.
21. N. Bao, T. T. Le, J.-X. Cheng and C. Lu, *Integrative Biology*, 2010, **2**, 113-120.
22. Y. Xia and G. M. Whitesides, *Angew Chem Int Ed*, 1998, **37**, 550-575.
23. I. K. Dimov, L. Basabe-Desmonts, J. L. Garcia-Cordero, B. M. Ross, A. J. Ricco and L. P. Lee, *Lab Chip*, 2011, **11**, 845-850.
24. M. A. Unger, H.-P. Chou, T. Thorsen, A. Scherer and S. R. Quake, *Science*, 2000, **288**, 113-116.
25. B. Harmon, B. R. Schudel, D. Maar, C. Kozina, T. Ikegami, C. T. Tseng and O. A. Negrete, *Journal of virology*, 2012.
26. V. V. Abhyankar and D. J. Beebe, *Analytical chemistry*, 2007, **79**, 4066-4073.
27. T. Ikegami, S. Won, C. J. Peters and S. Makino, *Journal of virology*, 2006, **80**, 2933-2940.
28. O. Ebert, K. Shinozaki, T. G. Huang, M. J. Savontaus, A. Garcia-Sastre and S. L. Woo, *Cancer research*, 2003, **63**, 3605-3611.
29. H. Boshra, G. Lorenzo, N. Busquets and A. Brun, *Journal of virology*, 2011, **85**, 6098-6105.
30. J. Reymann, N. Beil, J. Beneke, P. P. Kaletta, K. Burkert and H. Erfle, *BioTechniques*, 2009, **47**, 877-878.
31. J. Mercer, M. Schelhaas and A. Helenius, *Annual review of biochemistry*, 2010, **79**, 803-833.
32. C. Doil, N. Mailand, S. Bekker-Jensen, P. Menard, D. H. Larsen, R. Pepperkok, J. Ellenberg, S. Panier, D. Durocher, J. Bartek, J. Lukas and C. Lukas, *Cell*, 2009, **136**, 435-446.
33. B. Neumann, T. Walter, J. K. Heriche, J. Bulkescher, H. Erfle, C. Conrad, P. Rogers, I. Poser, M. Held, U. Liebel, C. Cetin, F. Sieckmann, G. Pau, R. Kabbe, A. Wunsche, V. Satagopam, M. H. Schmitz, C. Chapuis, D. W. Gerlich, R. Schneider, R. Eils, W. Huber, J. M. Peters, A. A. Hyman, R. Durbin, R. Pepperkok and J. Ellenberg, *Nature*, 2010, **464**, 721-727.